

Cite this: *RSC Adv.*, 2017, 7, 34669

## CO<sub>2</sub>-responsive self-healable hydrogels based on hydrophobically-modified polymers bridged by wormlike micelles†

Chunming Xiong,<sup>a</sup> Kang Peng,<sup>b</sup> Xiaofen Tang,<sup>a</sup> Zhengrong Ye,<sup>a</sup> Yang Shi<sup>a</sup> and Haiyang Yang<sup>ib</sup>\*<sup>b</sup>

CO<sub>2</sub>-responsive hydrogels, using CO<sub>2</sub> as a “green” trigger, have recently been of considerable interest. Herein, a novel CO<sub>2</sub>-responsive self-healable hydrogel is fabricated by simply mixing hydrophobically modified polyacrylamide (HMPAM) with sodium dodecyl sulfate (SDS)–*N,N,N',N'*-tetramethyl-1,3-propanediamine (TMPDA) surfactant micelles. In the presence of CO<sub>2</sub>, the SDS–TMPDA spherical micelles transform into long wormlike micelles, serving as multivalent cross-linkages to bridge HMPAM chains based on hydrophobic interactions. The interpenetrating three-dimensional network induces a sol-to-gel transition, accompanied by a 360 and 400 times enhancement of the zero-shear viscosity and storage modulus,  $G'$  ( $\omega = 6.28 \text{ rad s}^{-1}$ ), respectively. In addition, the sol–gel transition can be repeatedly and reversibly switched by cyclically bubbling and removing CO<sub>2</sub> without any harm. Furthermore, the CO<sub>2</sub>-responsive hydrogel exhibits significant shear-thinning and self-healing properties, suggesting that the hydrogel is injectable and could be used as a potential plug to block CO<sub>2</sub> gas breakthrough channels during CO<sub>2</sub> flooding. Therefore, we believe that the presented work will enable the development of the design of CO<sub>2</sub>-responsive self-healable hydrogels and their practical applications.

Received 8th June 2017

Accepted 5th July 2017

DOI: 10.1039/c7ra06418g

rsc.li/rsc-advances

## Introduction

Smart hydrogels that undergo physicochemical changes in response to external stimuli, such as pH,<sup>1–3</sup> light,<sup>4,5</sup> CO<sub>2</sub>,<sup>6–9</sup> thermal,<sup>10,11</sup> ionic strength<sup>12,13</sup> and electrical potential,<sup>14</sup> have been extensively explored as scaffolds for tissue engineering, carriers for controlled drug release, actuators and sensors in biomedical devices. Among them, CO<sub>2</sub>-responsive hydrogels are extremely important, and special, due to the “green” properties of CO<sub>2</sub>. CO<sub>2</sub> is a non-toxic, inexpensive, benign and abundant gas.<sup>15</sup> Moreover, using CO<sub>2</sub> as a trigger can lead to many switching cycles without the accumulation of byproducts.<sup>16,17</sup>

Up to now, CO<sub>2</sub>-responsive systems are generally categorized into three types based on their CO<sub>2</sub>-responsive groups: amidine, amine, and carboxyl groups.<sup>18</sup> Firstly, Jinying Yuan and co-workers<sup>19</sup> designed a specific amidine-containing diblock copolymer PEO-*b*-PAD to fabricate CO<sub>2</sub>-responsive polymeric vesicles with a biomimetic “breathing” feature. The size of these

vesicles over a wide range was tuned by CO<sub>2</sub>, which could control the degree of protonation of amidine species. Secondly, the group of Yue Zhao<sup>20</sup> demonstrated a novel polymer brush that exhibited CO<sub>2</sub>-controllable switching between extended (hydrated) and collapsed (dehydrated) chain conformations. Such CO<sub>2</sub>-switchable polymer solubility could be repeated many times without contamination of the solution by accumulated salts, unlike the conventional pH change induced by adding acids and bases. Thirdly, Viktor Fischer *et al.*<sup>21</sup> presented the synthesis of molecularly controlled carboxyl-functionalized nanoparticles, which could be coagulated by bubbling CO<sub>2</sub>.

Although CO<sub>2</sub>-responsive polymers have gained a rapid development over the last few years, some challenges still remain.<sup>22</sup> The amidine group is prone to hydrolysis in aqueous environments. CO<sub>2</sub>-responsive amphiphilic block copolymers require a demanding synthesis. For some latexes, the effective CO<sub>2</sub>-responsive behaviors only exist under a low solid content situation. Last but not least, CO<sub>2</sub>-responsive polymers are generally costly and hence have limitation in various applications. In particular, CO<sub>2</sub> flooding has become a significant technology for enhanced oil recovery (EOR). It is crucial to develop CO<sub>2</sub>-induced hydrogels *via* industrialization paths to efficiently plug CO<sub>2</sub> gas breakthrough channels to improve the sweep volume of CO<sub>2</sub>.<sup>23,24</sup>

On the other hand, the group of Yujun Feng reported three kinds of CO<sub>2</sub>-responsive surfactant-based self-assembled

<sup>a</sup>Research Institute of Science and Technology, China National Petroleum Corporation, Beijing, 100083, P. R. China

<sup>b</sup>CAS Key Laboratory of Soft Matter Chemistry, School of Chemistry and Materials Science, University of Science and Technology of China, Hefei, 230026, P. R. China. E-mail: yhy@ustc.edu.cn

† Electronic supplementary information (ESI) available. See DOI: 10.1039/c7ra06418g

structures (UC22AMPM, ODPTA, and SDS-TMPDA).<sup>25–27</sup> After treatment with CO<sub>2</sub>, free surfactants, vesicles, and spherical micelles switched to worm-like micelles in these systems, respectively. Inspired by previous studies<sup>28,29</sup> of the interaction between surfactants and hydrophobically modified polymers, we can apply these surfactant responders to endow the conventional responseless hydrophobically modified polyacrylamide (HMPAM) with fascinating CO<sub>2</sub>-responsive and self-healing properties.

Herein, a novel CO<sub>2</sub>-responsive self-healable hydrogel was fabricated by simply mixing HMPAM with sodium dodecyl sulfate (SDS)-*N,N,N',N'*-tetramethyl-1,3-propanediamine (TMPDA) surfactant micelles in aqueous solution. HMPAM was synthesized by free-radical micellar copolymerization of acrylamide, acrylic acid and *n*-dodecylmethacrylate, representing an important class of water-soluble associative polymers.<sup>30,31</sup> The SDS-TMPDA mixture was chosen, because CO<sub>2</sub> would protonate the tertiary amine groups the TMPDA molecules to induce a sphere-to-worm transition of SDS.<sup>27</sup> As shown in Fig. 1, SDS-TMPDA spherical micelles dissolved the HMPAM hydrogel in the absence of CO<sub>2</sub>. After bubbling CO<sub>2</sub> into the aqueous mixture, wormlike micelles formed, serving as multivalent cross-linkages to bridge HMPAM chains based on the hydrophobic interaction. The interpenetrating three-dimensional network induced a sol-to-gel transition, accompanied by 360 and 400 times the enhancement of zero-shear viscosity and storage modulus  $G'$  ( $\omega = 6.28 \text{ rad s}^{-1}$ ), respectively. The sol-gel transition could be repeatedly and

reversibly switched by cyclically bubbling and removing CO<sub>2</sub> without any residual chemicals such as salts which might be harmful to the performance of the hydrogel. More importantly, the CO<sub>2</sub>-responsive hydrogel exhibited significant shear-thinning and self-healing properties, suggesting that the hydrogel was injectable and could be used as the potential plug to block CO<sub>2</sub> gas breakthrough channels during CO<sub>2</sub> flooding. We believe that the presented work will provide a versatile and simple strategy for the design of CO<sub>2</sub>-responsive self-healable hydrogels, fostering their use in a wide range of applications such as enhanced oil recovery (EOR).

## Experimental section

### Materials

Acrylamide (AM), acrylic acid (AAc), sodium dodecyl sulfate (SDS), *N,N,N',N'*-tetramethyl-1,3-propanediamine (TMPDA) and ammonium persulfate (APS) were purchased from Sinopharm Chemical Reagent CO. Ltd. *n*-Dodecylmethacrylate (C12) was obtained from Aldrich. All the materials were used as received without further purification and experiments were performed using deionized (DI) water.

### Synthesis of hydrophobically modified polyacrylamide (HMPAM)

HMPAM was synthesized according to a previously reported method.<sup>29</sup> Briefly, 4.50 g SDS and 0.21 g C12 was dissolved in

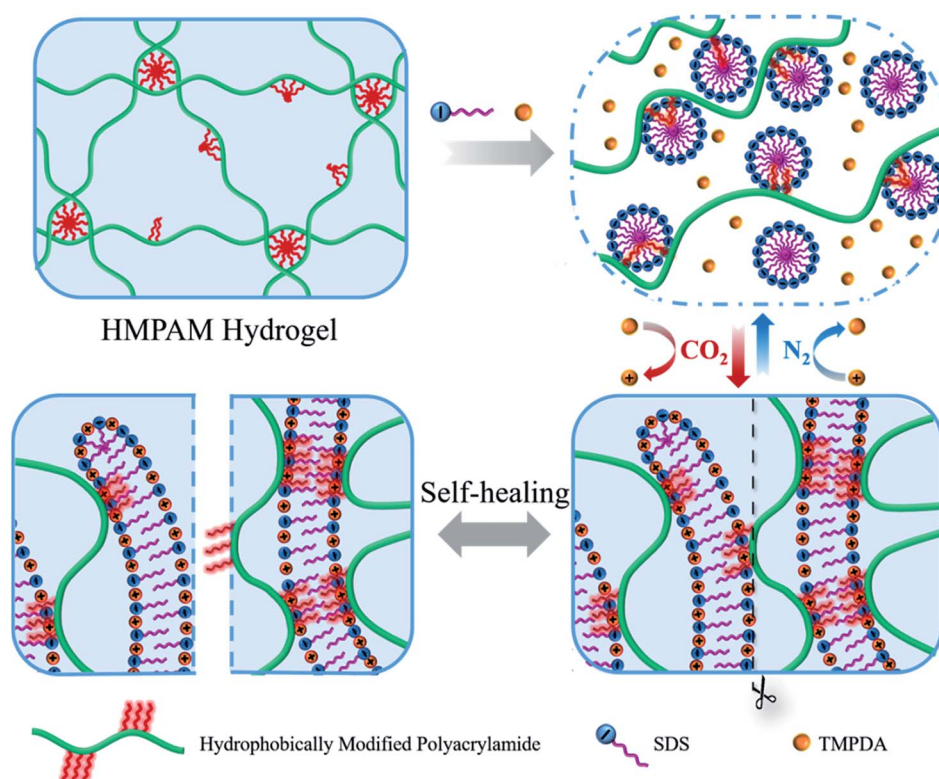


Fig. 1 Schematic illustration of the CO<sub>2</sub>-responsive sol-gel transition and the self-healing behavior of the hydrogels based on SDS-TMPDA wormlike micelles bridged HMPAM.



100.0 mL water to obtain an optically transparent solution. Then adding and dissolving 9.23 g AM and 0.50 g AAc with stirring for several minutes. Finally, 0.05 g APS initiated the copolymerization at 50 °C for 12 h under nitrogen. In the monomer feed, the molar fractions of AM, AAc and C12 were 94.4%, 5.0%, and 0.6%, respectively. After polymerization, the polymer was twice precipitated in a methanol/acetone mixture and dried in a vacuum at room temperature for 2 days.

### Sample preparation

Appropriate amounts of HMPAM were dissolved in DI water under vigorous stirring for 3 h. Then SDS–TMPDA was mixed with the HMPAM hydrogel for 1 h at room temperature. The molar ratio of SDS to TMPDA was fixed at 2 : 1. And the concentrations of SDS–TMPDA were given as the concentrations of TMPDA. After determining the phase behavior by visual inspection to have clear one-phase solutions, CO<sub>2</sub> was bubbled into the solutions at 25 °C with a fixed flow rate of 0.1 L min<sup>−1</sup> for 10 min under a pressure of 0.1 MPa for the gelation. Then the sample was equilibrated in a sealed vial for 24 h prior to subsequent tests. The formed hydrogel was converted to the sol state after removing CO<sub>2</sub> by bubbling N<sub>2</sub> at the same flow rate as for CO<sub>2</sub> at 75 °C for 30 min.

### Self-healing behavior

The hydrogel sample after preparation and equilibrium was cut in the middle, and then the two halves were stained with Rhodamine B (red dye) and Indigo carmine (blue dye), respectively. After merging the two pieces together for 60 s, the healed hydrogel could support its own weight.

### Rheological measurements

Rheological measurements were conducted on an ARG2 stress controlled rheometer (TA AR-G2) at 25 °C using a cone-plate of 40 mm diameter with a cone angle of 4°. The viscosity was measured as a function of shear rate for determining the zero-shear viscosity. The storage modulus ( $G'$ ) and loss modulus ( $G''$ ) were measured as a function of frequency within a linear viscoelastic regime, which was determined from the prior stress-sweep test.

To investigate the self-healing properties of the samples in response to applied shear forces, the samples were placed between the para-plate and the platform with special care. The following programmed procedure (applied shear force, expressed in terms of strain; duration in parentheses) was used: 1% (400 s) → 3500% (300 s) → 1% (400 s) → 3500% (300 s) → 1% (400 s) → 3500% (300 s) → 1% (400 s).

During all measurements, a solvent trap was used to minimize water evaporation.

## Results and discussion

### CO<sub>2</sub> responsiveness of the mixture of HMPAM and SDS–TMPDA

In our study, hydrophobically modified polymers consisted of a water-soluble poly(AM-co-AAc) backbone onto which a small

number of hydrophobic C12 alkyl chains were attached. Generally, the block distributed hydrophobic moieties from different polymer chains can associate and build a transitory three-dimensional network above the concentration of overlapping the coils.<sup>30,32</sup> Therefore, we firstly studied the effect of polymer concentrations on the HMPAM hydrogel. As depicted in Fig. 2a, the zero-shear viscosity (which was determined from the curve of viscosity *versus* shear rate in Fig. S1†) of HMPAM hydrogels showed an obvious increment with the polymer weight percentage increasing. Furthermore, from the curves of linear viscoelastic modulus,  $G'(\omega)$  and  $G''(\omega)$ , for the HMPAM hydrogel with various polymer weight percentages, it could be observed that the  $G'$  values had a substantial elastic response and were always larger than the  $G''$  values over the entire range of frequencies when the polymer weight percentage exceeded 0.3 wt% (Fig. S2†). These results indicated that more cross-linkages were constructed at a higher polymer concentration. Here, the polymer weight percentage was set as 2 wt% to obtain a hydrogel structure, as determined in Fig. 2b.

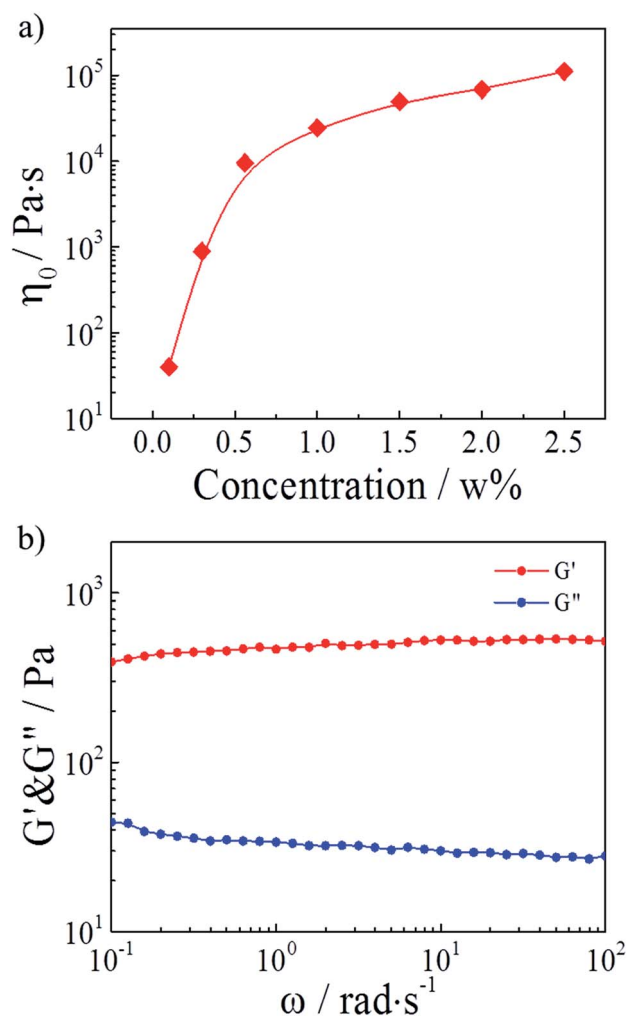


Fig. 2 (a) Zero-shear viscosity of HMPAM hydrogels as a function of the polymer weight percentage. (b) Linear viscoelastic modulus,  $G'(\omega)$  and  $G''(\omega)$ , for a 2 wt% HMPAM hydrogel.





Then, the combination with SDS–TMPDA micelles would endow the conventional responseless HMPAM hydrogel with fascinating CO<sub>2</sub>-responsive properties. The frequency dependencies of the storage modulus  $G'$  and the loss modulus  $G''$  were presented in Fig. 3a for the HMPAM hydrogel with various concentrations of SDS–TMPDA before bubbling CO<sub>2</sub>. When the concentration of SDS–TMPDA was relatively low (20 mM), the storage modulus  $G'$  exceeded the loss modulus  $G''$  in the whole frequency range, still indicative of a hydrogel structure. Increasing the concentration of SDS–TMPDA to 30 mM,  $G'$  and  $G''$  intersected, exhibiting viscoelastic behavior. Above 35 mM,  $G''$  was dominant over  $G'$ , implying that the HMPAM hydrogel was converted to the sol state. Meanwhile, the zero-shear viscosity dropped 3 orders of magnitude as increasing the concentration of SDS–TMPDA from 20 mM to 40 mM (Fig. S3†), which is consistent with the results on  $G'$  and  $G''$ . The gel-to-sol transition of HMPAM by mixing with SDS–TMPDA spherical micelles was attributed to the spherical micellar solubilisation of the hydrophobes.

After bubbling CO<sub>2</sub>, the frequency dependencies of the storage modulus  $G'$  and the loss modulus  $G''$  were presented in Fig. 3b. For all the concentrations of SDS–TMPDA, CO<sub>2</sub> induced stronger mechanical properties. Specifically speaking,  $G'$  was

increased by 2 to 3 orders of magnitude and behaved weakly frequency dependent in the whole frequency range investigated, when the concentration of SDS–TMPDA was 20 mM. For 30 mM and 35 mM,  $G'$  was dominant over  $G''$  over the entire frequency range, indicative of a predominantly elastic network rather than a viscous sol state. This elastic nature manifested that HMPAM chains were bridged by wormlike micelles based on the hydrophobic interaction. In other words, bubbling CO<sub>2</sub> would protonate the TMPDA molecules, leading to the formation of wormlike micelles which served as multivalent cross-linkages. However, for 40 mM,  $G'$  and  $G''$  intersected at a low frequency. As the concentration of SDS–TMPDA increasing, more wormlike micelles formed. It became less probable that an individual wormlike micelle contained side chains from several chains, suggesting the decrease in cross-linking density. Therefore, the mechanical properties of the hydrogel were correspondingly weakened. In Fig. S4,† the curves of viscosity *versus* shear rate for the HMPAM hydrogel with various concentrations of SDS–TMPDA after bubbling CO<sub>2</sub> also provided evidence of the interpretation.

Considering all the above results, the mixture of 2 wt% HMPAM and 35 mM SDS–TMPDA was selected as a representative sample for subsequent tests. Photographs demonstrating the CO<sub>2</sub>-responsive sol–gel transition were presented in Fig. 4a. After bubbling CO<sub>2</sub> into the aqueous mixture, wormlike micelles formed, serving as multivalent cross-linkages to bridge HMPAM chains based on the hydrophobic interaction. The interpenetrating three-dimensional network induced a sol-to-gel transition. Then the formed hydrogel could be converted to the initial sol state after removing CO<sub>2</sub> by bubbling N<sub>2</sub>.

As depicted in Fig. 4b, 360 times the enhancement of zero-shear viscosity was observed in the presence of CO<sub>2</sub>. In addition, the CO<sub>2</sub> induced hydrogel displayed a significant shear-thinning phenomenon. The viscosity remained almost constant up to a shear rate of 0.2 s<sup>−1</sup>, and then decreased more than 2 orders of magnitude with increasing shear rate. The dramatic change of viscosity indicated that the hydrophobes of HMPAM were pulled out of wormlike micelles under a high shear rate and the non-covalent interactions were considerably broken. For comparison, the curves of viscosity *versus* shear rate for the 35 mM SDS–TMPDA solution before and after bubbling CO<sub>2</sub> were measured in Fig. S5.†

As depicted in Fig. 4c, 400 times the enhancement of storage modulus  $G'$  ( $\omega = 6.28 \text{ rad s}^{-1}$ ) was observed in the presence of CO<sub>2</sub>. The sol-to-gel transition was determined by the frequency-sweep test. Generally,  $G' > G''$  indicated a solid-like response while  $G' < G''$  indicated a liquid-like response. Meanwhile, the frequency dependence was mainly attributed to the relative weak physical interaction of the supramolecular network. It was noteworthy that the 35 mM SDS–TMPDA solution still possessed a predominantly viscous nature after bubbling CO<sub>2</sub> (Fig. S6†). The  $G'$  and  $G''$  of the SDS–TMPDA solution before bubbling CO<sub>2</sub> were beyond the detection limit of the instrument.

### Reversibility of CO<sub>2</sub>-induced gelation

As a green trigger, CO<sub>2</sub> can lead to many switching cycles without the accumulation of byproducts. Thus, the reversible

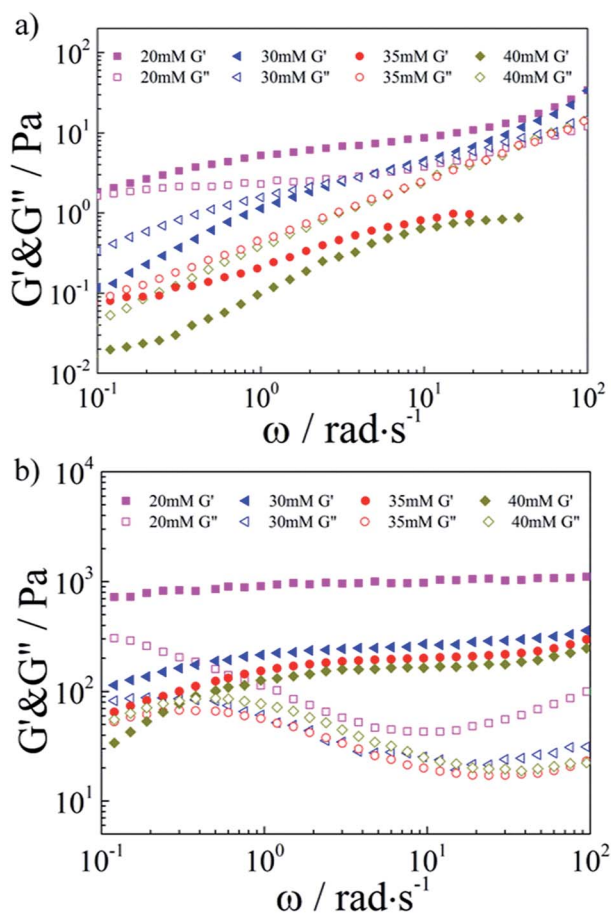


Fig. 3 Linear viscoelastic modulus,  $G'(\omega)$  and  $G''(\omega)$ , for the HMPAM hydrogel with various concentrations of SDS–TMPDA (a) before and (b) after bubbling CO<sub>2</sub>.



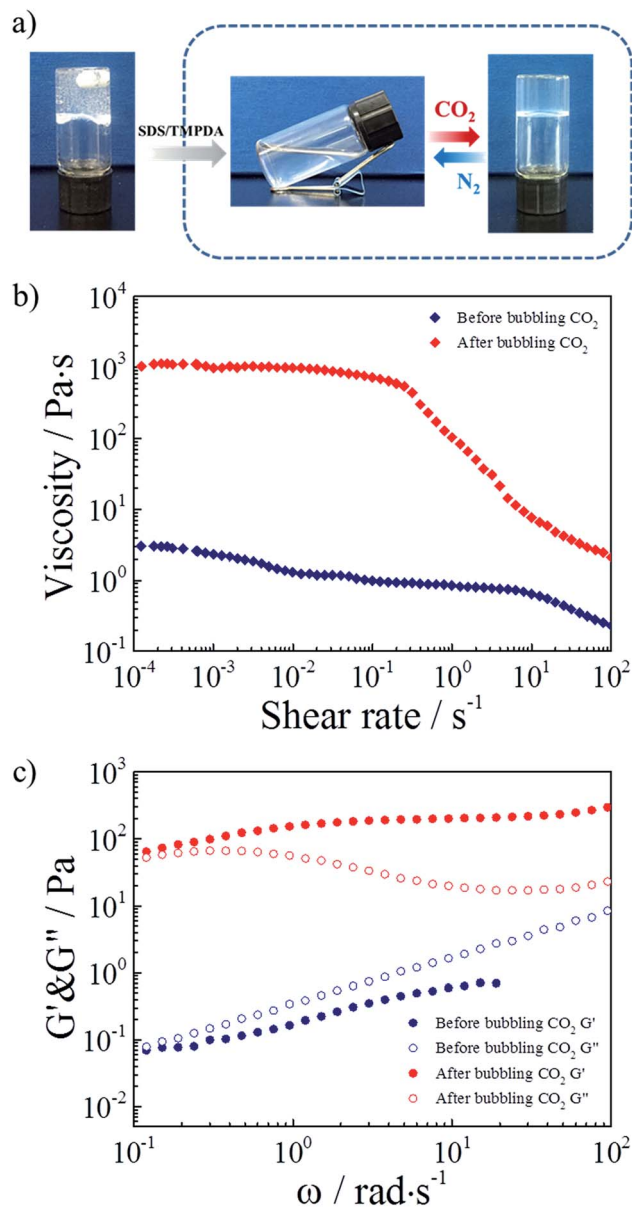


Fig. 4 (a) Photographs demonstrating the CO<sub>2</sub>-responsive sol-gel transition of the hydrogel based on SDS-TMPDA wormlike micelles bridged HMPAM. (b) Viscosity versus shear rate plots for the representative sample before and after bubbling CO<sub>2</sub>. (c) Linear viscoelastic modulus,  $G'(\omega)$  and  $G''(\omega)$ , for the representative sample before and after bubbling CO<sub>2</sub>.

switchability in rheological behaviors was evaluated next. As shown in Fig. 5a, the zero-shear viscosity of the hydrogel could be repeatedly and reversibly switched upon alternately bubbling CO<sub>2</sub> and N<sub>2</sub>. For more than four cycles, the change in the zero-shear viscosity was detected without any deterioration. Referring to the study of the research group of Yujun Feng, this finding could be explained that releasing CO<sub>2</sub> from the hydrogel by bubbling N<sub>2</sub> at 70 °C reconverted TMPDA to its initial non-ionic state, resulting in the collapse of wormlike micelles and the following destruction of the physically cross-linked network. On the other hand, Fig. 5b showed variation of the  $G'$  and  $G''$

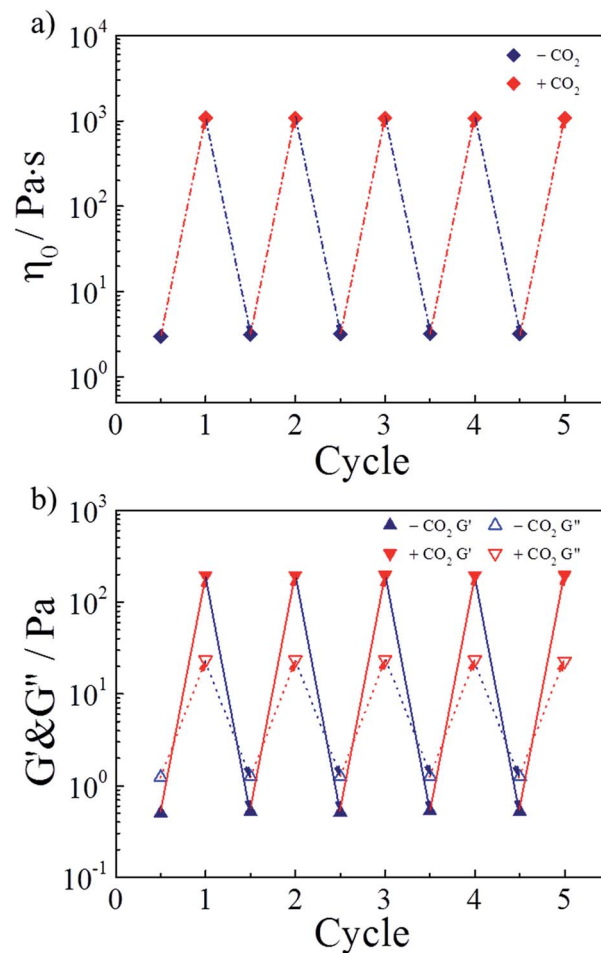


Fig. 5 Reversible switchability of (a) zero-shear viscosity and (b)  $G'$  and  $G''$  ( $\omega = 6.28 \text{ rad s}^{-1}$ ) for the representative sample upon alternate treatment of CO<sub>2</sub> and N<sub>2</sub>.

values of the invertible hydrogel during four cycles, further proving the perfect switchable ability.

### Self-healing study

Polymeric hydrogels capable of autonomous healing upon damage have numerous potential applications such as in drug delivery systems, artificial molecular tissues and oil industries.<sup>33–38</sup> SDS-TMPDA wormlike micelles not only endowed the HMPAM hydrogel with CO<sub>2</sub>-responsive properties but also the fascinating self-healing ability. It could be seen that the CO<sub>2</sub>-induced hydrogel sample merged into a whole without any cracks, after the equilibration in a sealed vial for 24 h, from the photograph in Fig. 4a. It was also observed that a large amount of cracks still appeared in the initial HMPAM hydrogel. Therefore, the self-healing property of the representative hydrogel sample was studied by following tests.

The self-healing ability was firstly demonstrated visually in Fig. 6a. Two pieces of hydrogel which were stained with different colors could self-repair into one integral piece within 60 s. And the healed hydrogel could support its own weight.



Then a strain sweep measurement was conducted on the presentative sample to test the influence of the strain. As depicted in Fig. 6b,  $G'$  was larger than  $G''$  (elastic-dominating) under small strain ( $\gamma < 100\%$ ). And the values of  $G'$  and  $G''$  kept constant, suggesting that the hydrogel network remained unaffected due to the intact cross-linkages. While the strain kept increasing, a gel to sol transition point ( $\gamma = 330\%$ ) occurred, implying that the hydrogel network was destroyed due to the disassociation of the cross-linkages at a high deformation strain.

Finally, repeated dynamic strain step tests ( $\gamma = 1\%$  or  $3500\%$ ) were carried out in Fig. 6c. It could be seen that a  $3500\%$

strain could completely inverted the  $G'$  and  $G''$  values, indicative of the deconstruction of the network. By returning the strain to  $1\%$ ,  $G'$  and  $G''$  recovered their original values rapidly, indicating the quick recovery of the inner network of the hydrogel. During the cyclic tests, this recovery behavior was significantly reversible. When SDS-TMPDA wormlike micelles were present, the hydrophobic moieties of the network chains could be solubilized and dynamically cross-linked.<sup>39,40</sup> After fracture, the hydrophobic units reversibly disengaged from the associations and easily found their partners in the other cut surface due to the hydrophobic interactions together with the help of the internal dynamics.<sup>31,41–43</sup> Therefore, the hydrogel exhibited the significant self-healing property within a short period of time.

## Conclusions

In conclusion, a novel  $\text{CO}_2$ -responsive self-healable hydrogel was fabricated by simply mixing HMPAM with SDS-TMPDA surfactant micelles in aqueous solution. After bubbling  $\text{CO}_2$ , wormlike micelles formed, serving as multivalent cross-linkages to bridge HMPAM chains based on the hydrophobic interaction. The interpenetrating three-dimensional network induced a sol-to-gel transition. Then removing  $\text{CO}_2$  could reconvert the hydrogel to its initial sol state. The sol-gel transition was repeatedly and reversibly switched by cyclically bubbling and removing  $\text{CO}_2$  without any harm. In addition, the  $\text{CO}_2$ -responsive hydrogel exhibited significant shear-thinning and self-healing properties, which allowed it to withstand repeated deformation and quickly recover its mechanical properties and structure. Therefore, we believe that the presented work should undoubtedly offer a universal and simple strategy to design  $\text{CO}_2$ -responsive self-healable hydrogels and provide new opportunities with regard to their practical applications such as smart fluids, intelligent delivery systems and a potential  $\text{CO}_2$  plugging agent for enhanced oil recovery (EOR) performed by  $\text{CO}_2$  flooding.

## Acknowledgements

This work was supported by the National Natural Science Foundation of China (Grant no. 51273189), the National Science and Technology Major Project of the Ministry of Science and Technology of China (2016ZX05016), and the National Science and Technology Major Project of the Ministry of Science and Technology of China (2016ZX05046).

## References

- 1 M. AngeláAleman-Garcia, *Chem. Sci.*, 2015, **6**, 4190–4195.
- 2 M. Krogsgaard, M. A. Behrens, J. S. Pedersen and H. Birkedal, *Biomacromolecules*, 2013, **14**, 297–301.
- 3 W. Xu, X. He, M. Zhong, X. Hu and Y. Xiao, *RSC Adv.*, 2015, **5**, 3157–3167.
- 4 K. Shi, Z. Liu, Y.-Y. Wei, W. Wang, X.-J. Ju, R. Xie and L.-Y. Chu, *ACS Appl. Mater. Interfaces*, 2015, **7**, 27289–27298.
- 5 Y.-Y. Xiao, X.-L. Gong, Y. Kang, Z.-C. Jiang, S. Zhang and B.-J. Li, *Chem. Commun.*, 2016, **52**, 10609–10612.

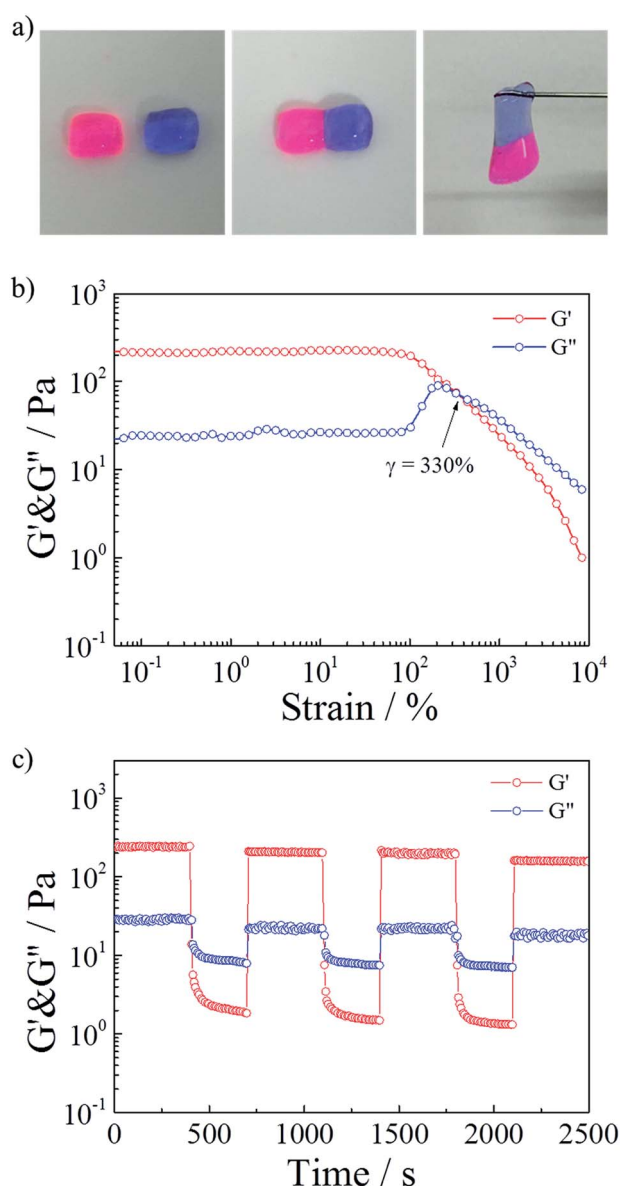


Fig. 6 (a) Two pieces of hydrogel, one was stained with Rhodamine B (red dye), one was stained with Indigo carmine (blue dye). The hydrogel were brought together for 60 s, and the healed hydrogel could support its own weight. (b) Storage modulus  $G'$  and loss modulus  $G''$  of a hydrogel as a function of strain. (c) Repeated dynamic strain step tests ( $\gamma = 1\%$  or  $3500\%$ ).



- 6 D. Han, O. Boissiere, S. Kumar, X. Tong, L. Tremblay and Y. Zhao, *Macromolecules*, 2012, **45**, 7440–7445.
- 7 Z. Guo, Y. Feng, Y. Wang, J. Wang, Y. Wu and Y. Zhang, *Chem. Commun.*, 2011, **47**, 9348–9350.
- 8 D. M. Rudkevich and H. Xu, *Chem. Commun.*, 2005, 2651–2659.
- 9 L. Zhang, J. Qian, Y. Fan, W. Feng, Z. Tao and H. Yang, *RSC Adv.*, 2015, **5**, 62229–62234.
- 10 C. Ma, Y. Shi, D. A. Pena, L. Peng and G. Yu, *Angew. Chem.*, 2015, **127**, 7484–7488.
- 11 L. Yu, W. Fu and Z. Li, *Soft Matter*, 2015, **11**, 545–550.
- 12 Z. Sun, F. Lv, L. Cao, L. Liu, Y. Zhang and Z. Lu, *Angew. Chem., Int. Ed.*, 2015, **54**, 7944–7948.
- 13 Z. Tao, K. Peng, Y. Fan, Y. Liu and H. Yang, *Polym. Chem.*, 2016, **7**, 1405–1412.
- 14 B. P. Lee and S. Konst, *Adv. Mater.*, 2014, **26**, 3415–3419.
- 15 T. Sakakura, J.-C. Choi and H. Yasuda, *Chem. Rev.*, 2007, **107**, 2365–2387.
- 16 Y. Liu, P. G. Jessop, M. Cunningham, C. A. Eckert and C. L. Liotta, *Science*, 2006, **313**, 958–960.
- 17 D. Han, X. Tong, O. Boissière and Y. Zhao, *ACS Macro Lett.*, 2011, **1**, 57–61.
- 18 S. Lin and P. Theato, *Macromol. Rapid Commun.*, 2013, **34**, 1118–1133.
- 19 Q. Yan, R. Zhou, C. Fu, H. Zhang, Y. Yin and J. Yuan, *Angew. Chem.*, 2011, **123**, 5025–5029.
- 20 S. Kumar, X. Tong, Y. L. Dory, M. Lepage and Y. Zhao, *Chem. Commun.*, 2013, **49**, 90–92.
- 21 V. Fischer, K. Landfester and R. Munoz-Espi, *ACS Macro Lett.*, 2012, **1**, 1371–1374.
- 22 H. Liu, S. Lin, Y. Feng and P. Theato, *Polym. Chem.*, 2017, **8**, 12–23.
- 23 G. Yuncong, Z. Mifu, W. Jianbo and Z. Chang, *Pet. Explor. Dev.*, 2014, **41**, 88–95.
- 24 D.-X. Li, L. Zhang, Y.-M. Liu, W.-L. Kang and S.-R. Ren, *Pet. Sci.*, 2016, **13**, 247–258.
- 25 Y. Zhang, Z. Chu, C. A. Dreiss, Y. Wang, C. Fei and Y. Feng, *Soft Matter*, 2013, **9**, 6217–6221.
- 26 Y. Zhang, Y. Feng, J. Wang, S. He, Z. Guo, Z. Chu and C. A. Dreiss, *Chem. Commun.*, 2013, **49**, 4902–4904.
- 27 Y. Zhang, Y. Feng, Y. Wang and X. Li, *Langmuir*, 2013, **29**, 4187–4192.
- 28 X. Hao, H. Liu, Y. Xie, C. Fang and H. Yang, *Colloid Polym. Sci.*, 2013, **291**, 1749–1758.
- 29 X. Hao, H. Liu, Z. Lu, Y. Xie and H. Yang, *J. Mater. Chem. A*, 2013, **1**, 6920–6927.
- 30 F. Candau and J. Selb, *Adv. Colloid Interface Sci.*, 1999, **79**, 149–172.
- 31 D. C. Tuncaboylu, A. Argun, M. Sahin, M. Sari and O. Okay, *Polymer*, 2012, **53**, 5513–5522.
- 32 E. K. Penott-Chang, L. Gouveia, I. J. Fernández, A. J. Müller, A. Diaz-Barrios and A. E. Saez, *Colloids Surf., A*, 2007, **295**, 99–106.
- 33 M. Nakahata, Y. Takashima, H. Yamaguchi and A. Harada, *Nat. Commun.*, 2011, **2**, 511.
- 34 U. Gulyuz and O. Okay, *Soft Matter*, 2013, **9**, 10287–10293.
- 35 H. Meng, P. Xiao, J. Gu, X. Wen, J. Xu, C. Zhao, J. Zhang and T. Chen, *Chem. Commun.*, 2014, **50**, 12277–12280.
- 36 Y. Yang and M. W. Urban, *Chem. Soc. Rev.*, 2013, **42**, 7446–7467.
- 37 H. Liu, C. Xiong, Z. Tao, Y. Fan, X. Tang and H. Yang, *RSC Adv.*, 2015, **5**, 33083–33088.
- 38 A. Phadke, C. Zhang, B. Arman, C.-C. Hsu, R. A. Mashelkar, A. K. Lele, M. J. Tauber, G. Arya and S. Varghese, *Proc. Natl. Acad. Sci. U. S. A.*, 2012, **109**, 4383–4388.
- 39 D. C. Tuncaboylu, M. Sari, W. Oppermann and O. Okay, *Macromolecules*, 2011, **44**, 4997–5005.
- 40 D. C. Tuncaboylu, M. Sahin, A. Argun, W. Oppermann and O. Okay, *Macromolecules*, 2012, **45**, 1991–2000.
- 41 A. Argun, M. P. Algi, D. C. Tuncaboylu and O. Okay, *Colloid Polym. Sci.*, 2014, **292**, 511–517.
- 42 U. Gulyuz and O. Okay, *Macromolecules*, 2014, **47**, 6889–6899.
- 43 G. Akay, A. Hassan-Raeisi, D. C. Tuncaboylu, N. Orakdogan, S. Abdurrahmanoglu, W. Oppermann and O. Okay, *Soft Matter*, 2013, **9**, 2254–2261.

